

Global Elastic Response Simulation

Project Representative

Seiji Tsuboi

Data Research Center for Marine-Earth Sciences, Japan Agency for Marine-Earth Science and Technology

Authors

Satoru Tanaka

Institute for Research on Earth Evolution, Japan Agency for Marine-Earth Science and Technology

Seiji Tsuboi

Data Research Center for Marine-Earth Sciences, Japan Agency for Marine-Earth Science and Technology

In this project, we pursue accurate numerical techniques to obtain theoretical seismic waves for realistic three dimensional (3-D) Earth models using Spectral-Element Method. We calculate synthetic seismic waveform for 2011 Tohoku earthquake (Mw9.0) using fully 3-D Earth model. Our results indicate that the earthquake rupture model we have used for this simulation is fairly accurate to grasp the rupture propagation along the earthquake fault. We also have calculated synthetic seismograms for Fiji deep earthquake and compared with the observed seismograms recorded in continental China. The results demonstrate that current 3D mantle seismic velocity model does not reproduce anomalous seismic shear waves reflected at the core-mantle boundary.

Keywords: Synthetic seismograms, 3-D velocity structure of the Earth, Spectral Element Method, Core-mantle structure

1. 2011 Tohoku earthquake

1.1 Earthquake rupture mechanism

Last year we have used finite source rupture model for 2011 Tohoku earthquake obtained by the same approach of Nakamura et al., 2010 [1] to compute synthetic seismograms. Instead we use another finite source model of Lee et al (2011) [2] to assess the effect of different source model on the synthetics, this year. The rupture model of Lee et al (2011) assumes that the strike of the fault plane is 193 degree and the dip is 14 degree. They used teleseismic, local strong motion and near-field coseismic geodetic data to investigate the source rupture process. The assumed fault length is totally 400 km consistent with the aftershock distribution. They modeled the rupture process by using 9560 point sources distributed over the fault surface. The largest asperity developed around the hypocenter with a maximum slip over 50 m. This asperity covered a broad area of about $200 \times 200 \text{ km}^2$. Its slip concentrated in two areas, one around the hypocenter at a depth between 10–50 km, and the other located slightly north from the hypocenter between about 10–30 km depth. These two areas are highly overlapped on the largest one. The other two secondly large asperities appeared to the south and north from the hypocenter and were at depths of 10–40 km and 10 km, respectively. Rupture properties on these asperities are both thrust predominately. The total amount of the released seismic moment corresponds to moment magnitude Mw=9.0. The duration of source time function is 160 sec. The fault length of 400 km and the source duration time of 160 sec are typical for Mw 9.0 earthquake. However, the maximum

slip of 49 m is unusually large. There are many rupture models for this earthquakes and we examine the validity of these fault rupture parameters by comparing the theoretical seismograms computed for this fault model with the observed seismograms.

1.2 Broadband synthetic seismograms

We calculate broadband synthetic seismograms with this source propagation model for a realistic 3D Earth model using the spectral-element method (Komatitsch and Tromp, 2002 [3]). The simulations are performed using 1014 processors, which require 127 nodes of the Earth Simulator 2. We use a mesh with 200 million spectral-elements, for a total of 13 billion global integration grid points. This translates into an approximate grid spacing of 2.0 km along the Earth's surface. On this number of nodes, a simulation of 30 minutes of wave propagation accurate at periods of 3.5 seconds and longer requires about 6 hours of CPU time. An example of waveform matches are shown in Fig. 1, where three component broadband seismograms are compared with the observations at teleseismic stations, AFI (Afiamalu, Samoa Islands, epicentral distance 67 degrees), and for ESK (Edinburgh, U.K., 81 degrees) in Fig. 2. Each trace is bandpass filtered between 0.002 Hz and 0.1 Hz. We may say that the synthetic seismograms reproduces observed seismograms generally well for body waves. Although surface waves are not modeled well, but it is because the surface waves with this period range depend on shallow crustal structure, which may not be modeled well in the 3D mantle model. These results indicate that the synthetic seismograms computed for this finite

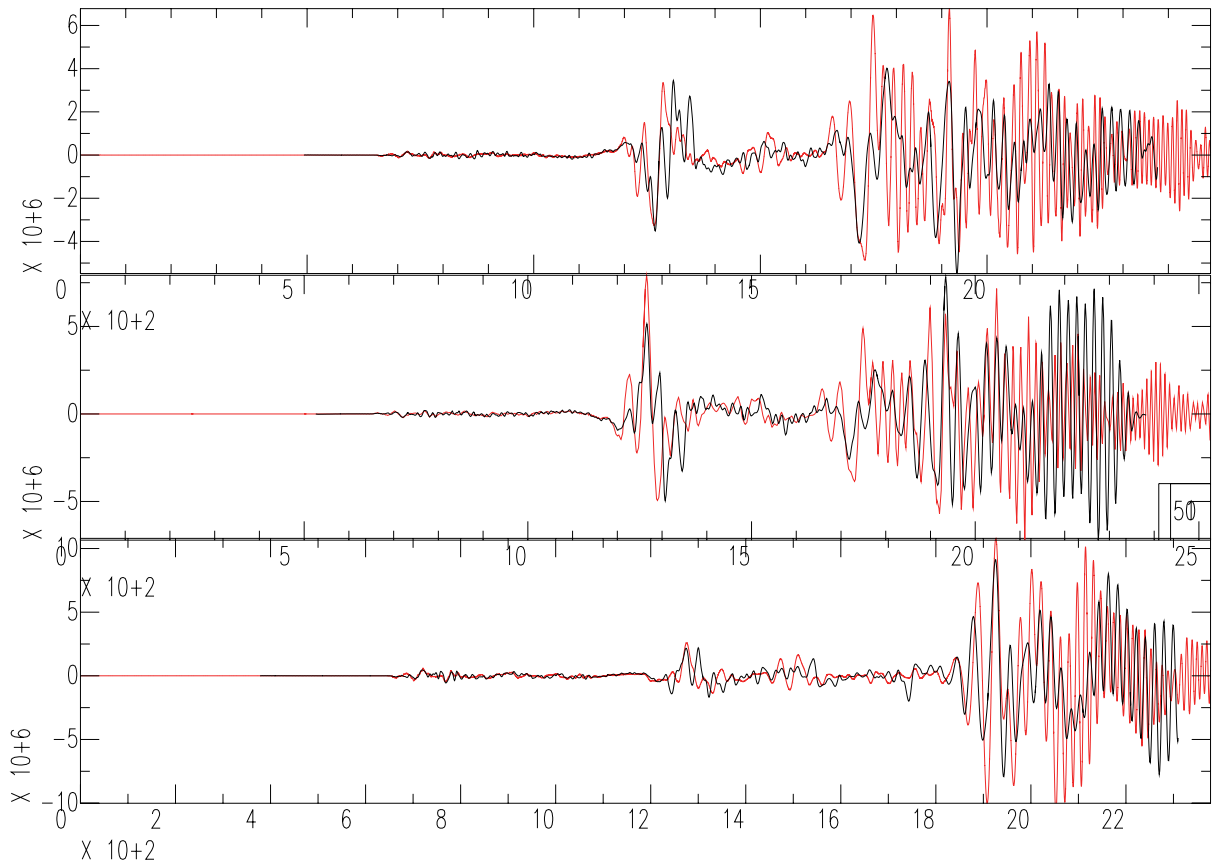


Fig. 1 Comparisons of synthetic seismograms and observaion for IRIS GSN station AFI , where the epicentral distances are 67 degree. The synthetics and the observations are in red and black, respectively. Instrument responses are convolved to synthetics to convert them to ground velocity. Traces are EW, NS, and UD components from top to bottom, respectively. The origin of the time axis is origin time of the event and the vertical axis shows digital count. All of the traces are bandpass filtered between 500 sec and 10 sec.

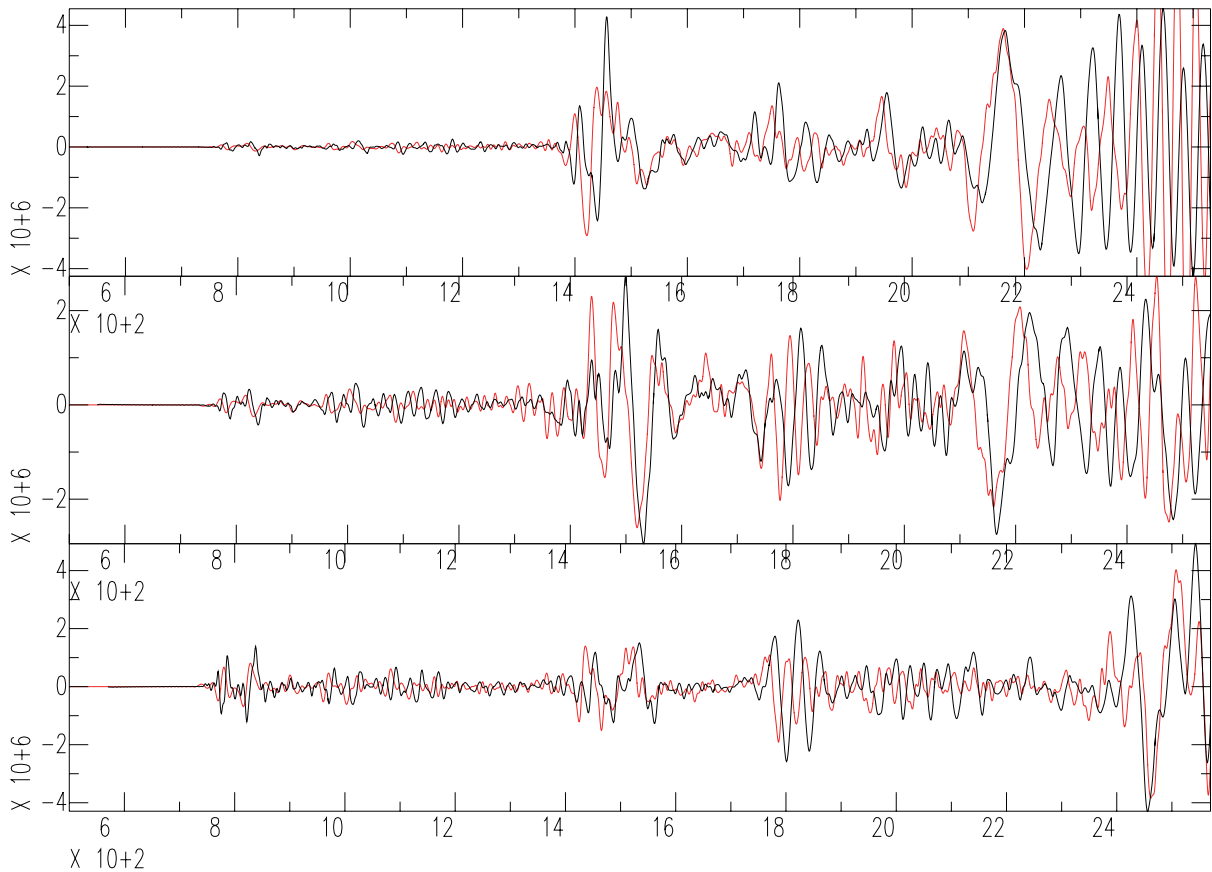


Fig. 2 Comparison of synthetic seismograms and observation for IRIS GSN station ESK, where the epicentral distance is 92 degree.

source model reproduce observed seismograms for teleseismic stations, which suggest that this source model captures rupture properties of this earthquake. The synthetics computed for Lee et al (2011)'s model generally reproduces features of observed seismograms and show improvements compared with the results we did last year, which imply that the differences of rupture model may be distinguishable by comparing synthetics with the observed seismograms

2. Differential travel times of S and ScS phases of a Fiji earthquake recorded by NECESSArray

2.1 NECESSArray

NECESSArray is a large-scale temporal seismic network deployed in the Northeastern China since September 2009 to August 2011, which is the abbreviation of NorthEast China Extended SeiSmic Array (Fig. 3a). The primary objective of NECESSArray is to examine the fate of the Pacific plate [Fukao

et al., 2009][4] and the structure of the crust and upper mantle beneath China. Also NECESSArray is a powerful tool for the study of the deep Earth structure. Here we show a preliminary result for the lower mantle study.

2.2 Data and Method

S and ScS phases from a Fiji deep earthquake (its epicenter is marked by the open star in Fig. 3a) are examined, of which typical ray paths on the vertical great circle between the source and the middle of the array are presented in Figs. 3b and 3c. The background color indicates the shear velocity perturbation taken from a global model of S20RTS [Ritsema et al., 1999] [5] and its variation. Interestingly, the bounce points of ScS phases at the core-mantle boundary are located around the edge of the Large Low Shear Velocity Province (LLSVP) [Garnero, 2000][6] beneath the Pacific Ocean (Fig. 3b). The travel times of ScS-S are compared with those measured on seismograms

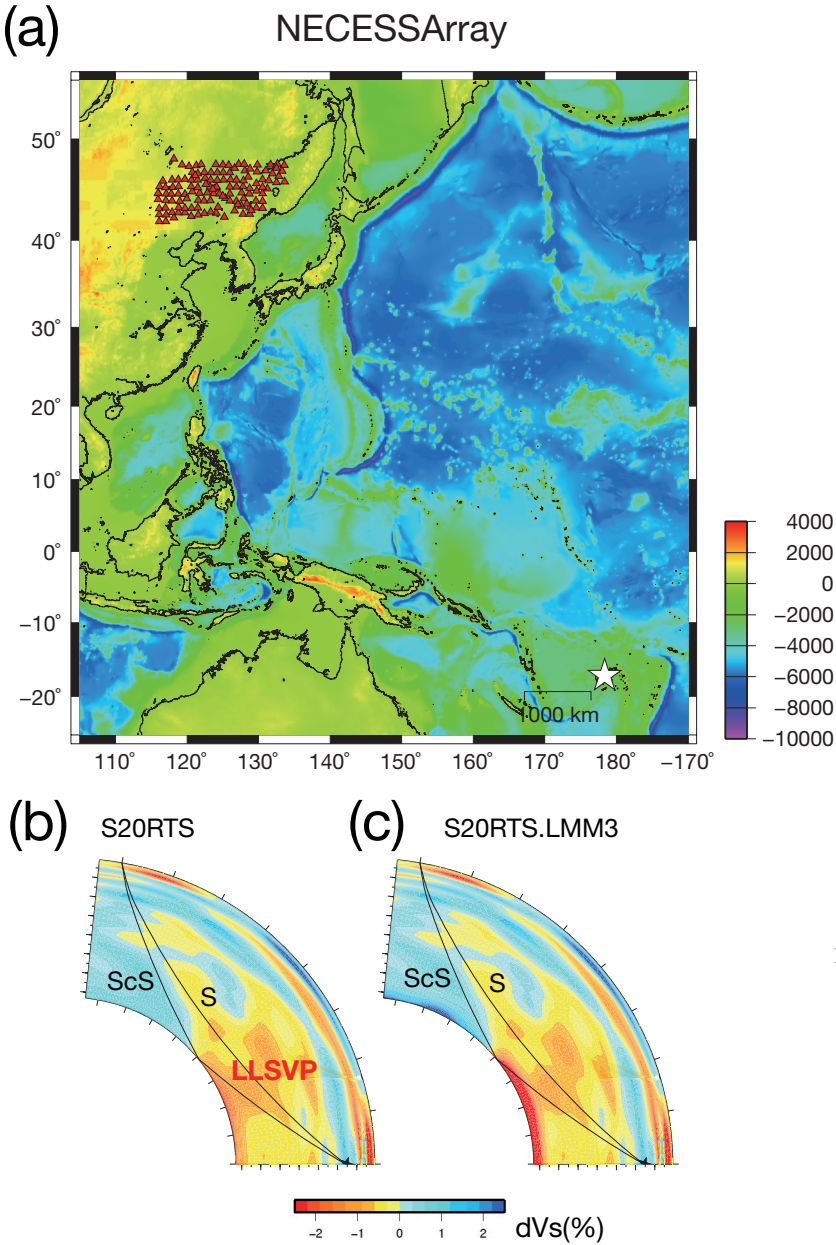


Fig. 3 (a) A topographic map of the eastern Asia and Western Pacific Ocean. Small triangles are the seismic stations of NECESSArray. The open star is the epicenter of a Fiji deep earthquake occurred on 9th November, 2009. The ray paths of S and ScS phases are plotted on the vertical cross-section between the hypocenter and the middle of NECESSArray with the velocity perturbations of (b) S20RTS and (c) S20RTS.LMM3.

calculated by the spectral element method (SEM) [Komatitsch and Tromp, 2002][3] implemented in the Earth Simulator. The SEM can synthesize seismograms involving topography, three-dimensional crustal (Crust2.0) [Bassin et al., 2000] [7] and mantle (S20RTS, Fig.3b) structures. As the velocity perturbations near the CMB in global tomography models are usually smoothed and underestimated, we modify the implemented model in which the spherical harmonic coefficients for the lowermost mantle are multiplied by factor 3 as shown in Fig. 3c (S20RTS.LMM3).

2.3 Results and Discussion

Figures 4a-d show the observed and synthetic seismograms by PREM, S20RTS, and S20RTS.LMM3 with a band-pass filter with cut-off periods of 20 and 50 s, respectively. The seismograms are aligned on the theoretical travel times of S phases. The red lines show the peak amplitudes for ScS phases. We read the peaks of S and ScS phases to determine the ScS–S differential travel times, which are plotted as a function of epicentral distance (Fig. 5). The observed differential travel times are much larger than those obtained by PREM and their differences are almost constant in the observable distance range, while the differential travel times by S20RTS and S20RTS.LMM3.

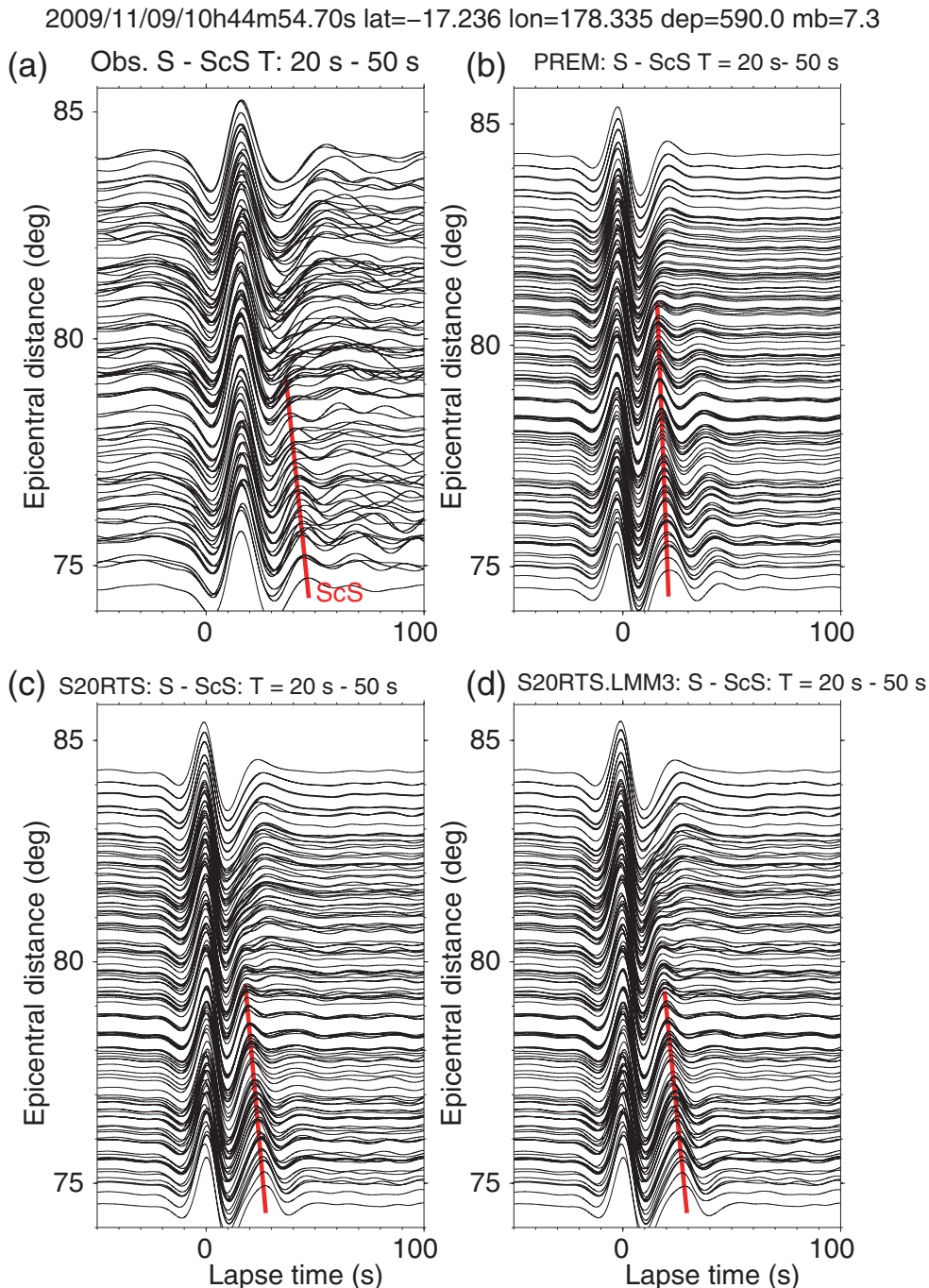


Fig. 4 Seismic record sections including S and ScS phases for (a) observed waveforms, and synthetic ones of (b) PREM, (c) S20RTS, and (d) S20RTS.LMM3. The travel times are aligned on the theoretical travel times of S phases. Red lines indicate the peak locations of ScS phases.

LMM quickly decrease and coincide with those by PREM at the distances greater than 78°. Thus further modeling is required to explain the observation, especially the extension of the low velocity region toward the northwest and the amount of the velocity reduction are highly interested.

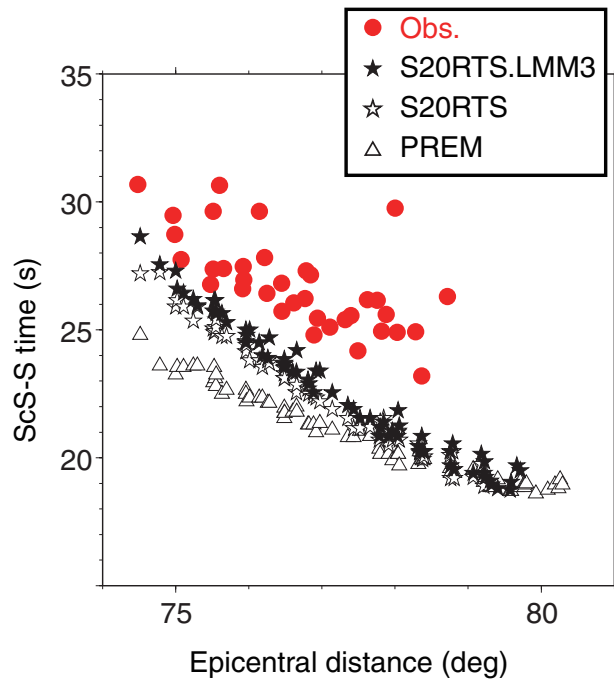


Fig. 5 Differential travel times of S and ScS phases as a function of epicentral distance. Red circles, close and open stars, and open triangles mean those obtained from the observed seismograms, those calculated with S20RTS.LMM3, S20RTS, and PREM, respectively.

References

- [1] Nakamura, T., Tsuboi, S., Kaneda, Y., and Yamanaka, Y., 2010. Rupture process of the 2008 Wenchuan, China earthquake inferred from teleseismic waveform inversion and forward modeling of broadband seismic waves, *Tectonophysics*, 491, 72-84.
- [2] Lee, S. J., B. S. Huang, M. Ando, H. C. Chiu, and J. H. Wang, 2011. Evidence of large scale repeating slip during the 2011 Tohoku-Oki earthquake, *Geophys. Res. Lett.*, 38, L19306.
- [3] Komatitsch, D. and Tromp, J., 2002. Spectral-element simulations of global seismic wave propagation-I. Validation, *Geophys. J. Int.*, 149, 390-412.
- [4] Fukao, Y., M. Obayashi, and T. Nakakuki, 2009. Stagnant Slab: A Review, *Ann. Rev. Earth Planet. Sci.*, 37(1), 19-46, doi:10.1146/annurev.earth.36.031207.124224.
- [5] Ritsema, J., H. J. van Heijst, and J. H. Woodhouse, 1999. Complex shear wave velocity structure imaged beneath Africa and Iceland, *Science*, 286(5446), 1925-1928.
- [6] Garnero, E. J., 2000. Heterogeneity of the lowermost mantle, *Ann. Rev. Earth Planet. Sci.*, 28, 509-537.
- [7] Bassin, C., G. Laske, and G. Masters, 2000. The Current Limits of Resolution for Surface Wave Tomography in North America, *EOS, Trans. Am. Geophys. Un.*, 81, F897.

全地球弾性応答シミュレーション

プロジェクト責任者

坪井 誠司 海洋研究開発機構 地球情報研究センター

著者

田中 聡 海洋研究開発機構 地球内部ダイナミクス領域

坪井 誠司 海洋研究開発機構 地球情報研究センター

スペクトル要素法により現実的な3次元地球モデルに対する理論地震波形記録を2011年東北地方太平洋沖地震(Mw9.0)に対して計算した。計算は地球シミュレータの127ノードを用いて、周期約5秒の精度で行った。計算した理論地震波形は観測波形をよく説明しており、用いた地震断層モデルがよく断層における破壊過程をモデル化していることを示している。計算した地震波形は断層破壊モデルの違いにより特徴が異なり、観測波形との比較により破壊モデルの決定する分解能が十分であることが分かった。

フィジーで起きた深発地震により励起された地震波を中国大陸に展開された地震計アレイで観測した波形に対してスペクトル要素法による理論地震波形計算を行った。観測された波形には核マントル境界で反射されたS波について、既存のマントル構造モデルでは説明できない到着時を示すものがあることが分かった。これにより核マントル境界のS波構造をより詳細に決定出来る可能性があることが分かった。

キーワード:理論地震波形記録, 3次元地球内部構造, スペクトル要素法, 核マントル境界